

MEASUREMENT OF DIFFUSION COEFFICIENT
USING LASER INTERFEROMETRIC TECHNIQUE

by

445

ROMESHEHAI V. AMIN

B. Sc., Maharaja Sayajirao University, 1959

B. S., University of Missouri School of
Mines and Metallurgy, 1962

A MASTER'S THESIS

submitted in partial fulfillment of the
requirements of the degree

MASTER OF SCIENCE

Department of Chemical Engineering

KANSAS STATE UNIVERSITY

Manhattan, Kansas

1966

Approved by:

Langston Fan

Major Professor

LD
266F
T4
1966
A 517
C. 2
Document

TABLE OF CONTENTS

INTRODUCTION	1
LITERATURE SURVEY	4
MATERIALS AND METHOD	13
Materials	13
Method	14
Apparatus	19
Experimental Method	23
Calculation of Observed Diffusion Coefficient	25
Zero-time Correction of Observed Diffusion Coefficient	31
PRESENTATION AND DISCUSSION OF EXPERIMENTAL RESULTS	33
CONCLUSIONS	51
RECOMMENDATIONS	53
ACKNOWLEDGMENTS	55
LIST OF SYMBOLS USED	56
LITERATURE CITED	58
APPENDIX	60
I. Integration of Equation (15)	60
II. Solution of Fick's Second Law Satisfying Initial and Boundary Conditions	62

III. Differentiation of Solution of Fick's Second Law With Respect to x	64
IV. Description of Leeds and Northrup Automatic Recording Microphotometer	66
V. Flow Sheet and Computer Program for Statistical Treatment of Experimental Data	70
VI. Sample Data Sheet and Sample Calculations	76

INTRODUCTION

Theoretical and practical interest in liquid diffusion has been maintained for over a century. Since the diffusion process is one of the aspects of liquid behavior which must be described by a satisfactory liquid-state theory, observed diffusion rates have been useful in both formulating and testing such theories. Even though liquid diffusion is one of the rate controlling factors in various mass-transfer operations, the diffusivities of fewer than 500 systems have been reported till 1960 (1).

The main reason for the lack of experimental results is the excessive time required for measuring diffusion coefficients. Furthermore, most of the methods employed to measure diffusion coefficients require tedious and difficult measurements of concentration or other concentration-dependent physical quantities.

One of the latest developments in the methods for measuring diffusion coefficients is the measurement of the refractive index gradient by use of the optical wedge diffusion cell. This technique developed by Nishijima and Oster (2) is best suited to systems in which the refractive index is a linear function of concentration. The time for diffusion required in this method is of the order of minutes rather than hours or days as in other methods.

The studies in this thesis were conducted to find the equipment best suited for the adaptation of the technique of Nishijima and Oster (2). The major change from the conventional equipment of Nishijima and Oster was the use of a laser beam as a source of monochromatic light for obtaining the interference fringes. The equipment was tested by obtaining the diffusion coefficient at one concentration in the intermediate concentration range of an aqueous sucrose solution. This intermediate sucrose concentration range was selected because of the following two reasons:

(1) The diffusion data in the intermediate sucrose concentration range were unavailable in the literature. Whereas, the diffusion data in the extremely dilute sucrose concentration range (below 0.06 g sucrose/ml of solution) were reported by Goesting and Morris (3) and in the supersaturated sucrose concentration (in the vicinity of 0.80 g sucrose/ml of solution) by English and Dole (4). The linear concentration-dependence of the diffusion coefficients was indicated in the ranges studied by these authors.

(2) The refractive index data for the whole sucrose concentration range were available in the Handbook of Physics and Chemistry (5). For a small range of concentration, the refractive index was a linear function of concentration. Also, if different volumes of the two diffusing solutions were used, then the final average concentration of the system could be found by measuring the refractive

index with a refractometer. This would avoid the necessity of exact measurements of the volume of the solutions used.

LITERATURE SURVEY

Because diffusivities are generally reported in terms of experimental observations on a somewhat arbitrary basis, it is worthwhile to review in some detail an elementary picture of the diffusion process and the development of the basic diffusion equations. In the usual sense, diffusion of mass refers to the dissipation of a concentration gradient by molecular transfer with no overall mass flow caused by external forces. To visualize the reasons for this observed motion, consider the behavior of a solute molecule in a given solution. The energy possessed by the molecules in the liquid state caused the solute molecule to collide constantly with solvent molecules, and in a more concentrated solution, also with other solute molecules. These collisions keep the solute molecule in a state of random motion, each individual collision moving it without regard for any concentration gradient present. While it is possible to calculate the mean distance which a molecule would travel in a given time interval, there is no way of predicting its actual path. A plot of probable position with time would be a series of concentric circles about its initial position.

In view of the apparent statistical behavior inherent in the diffusion process, it should be possible to relate unordered molecular

motion to diffusion flow. The first successful attempt was made by Einstein (6) in his discussion of Brownian motions.

The first successful mathematical formulation of diffusion rates was given by Fick (6) who deduced forces in the diffusion process analogous to those in heat flow. He observed that for a given temperature and pressure, the rate of transfer appeared to be proportional only to the concentration gradient. This simple relation, now well known as Fick's first law, for unidirectional diffusion may be written as (6)

$$J = -D \frac{dc}{dx} \quad (1)$$

where J is the rate of mass transfer per unit area and dc/dx is the concentration gradient. The diffusion coefficient D is presumed to be constant for a given system, and the negative sign indicates that the flow is in the opposite direction to the direction of the concentration gradient.

For mathematical analysis of diffusion experiments, it is convenient to transform Fick's first law into a form known as Fick's second law. By combining equation (1) with the requirements of a continuity of mass over a differential volume element of unit cross-section, Fick's second law can be written as (6)

$$\frac{\partial c}{\partial t} = D \left(\frac{\partial^2 c}{\partial x^2} \right) \quad (2)$$

where D is considered to be independent of concentration. In a more general case where D is a function of concentration, equation (2) can be rewritten as

$$\frac{\delta c}{\delta t} = \frac{\delta}{\delta x} \left(D \frac{\delta c}{\delta x} \right). \quad (3)$$

The number of experimental methods based on Fick's first law is restricted. It is possible to measure the diffusion flux in a given system with a known concentration gradient. For the given flux the value of D is immediately calculable from equation (1)

$$D = -J / (dc/dx) \quad (4)$$

It is possible to integrate the above expression if D is assumed to be constant and the concentration to be a linear function of distance. An excellent review of the methods based on Fick's first law has been presented by Johnson and Babb (6).

For the solutions based on Fick's second law, although D is about invariably concentration-dependent, many methods can be utilized over sufficiently small concentration ranges so that D can be considered constant. In addition, many methods will yield a value of D equal to the true differential coefficient for the mean of the concentrations used if D is assumed to be a linear function of concentration over the range under study. The number of geometric possibilities useful in the diffusion study based on Fick's second law is mentioned by Jost (7) and Crank (8). The one for an infinite

cylinder with given initial and boundary conditions will be reviewed here in detail, since it is the basis for the experimental method used in this study.

Consider a system in which a solution of concentration c'_0 is in contact with another solution of concentration c''_0 is shown in Figure 1(a). The boundary between the two solutions is at a point $x=0$ and positive values are assigned to x in the direction of increasing concentration c'_0 . It will be assumed that no external force except that of osmosis is acting on the solute molecules and that the solute concentration is in the "ideal solution" range.

For the condition stated above the solution of equation (2) must fulfill the following sets of conditions:

$$\text{Initial } f(x) = c'_0 \quad @ \ x > 0 \quad @ \ t \leq 0; \quad f(x) = c''_0 \quad @ \ x < 0 \quad @ \ t \leq 0 \quad (5a)$$

$$\text{Boundary } c = c'_0 \quad @ \ x = +\infty \quad @ \ t = t; \quad c = c''_0 \quad @ \ x = -\infty \quad @ \ t = t \quad (5b)$$

Using the method of variable separation (9) the solution of equation (2) satisfying the conditions given by equations (5a) and (5b) is

$$c(x, t) = F(x)G(t) \quad (6)$$

where F and G are functional representations.

Differentiation and substitution of equation (6) into equation (2) yields

$$\dot{F}G = DF''G \quad (6a)$$

where dots denote derivatives with respect to t , and primes denote

derivatives with respect to x . Dividing equation (6a) by DFG yields

$$\frac{\dot{G}}{DG} = \frac{F''}{F} \quad (6b)$$

The expression on the left hand side of equation (6b) depends only on t , while the right hand side depends only on x . Hence, both expressions must be equal to a constant, say k . If the expression on the left hand side is not constant, then changing t will presumably change the value of this expression but certainly not that of the right hand side, since the latter does not depend on t . A similar argument holds for the proof of independence of equation (6b) with respect to x . Consideration of the above arguments yields the two ordinary linear differential equations. For $k=0$ the only solution $C=FG$ that satisfies the conditions given by equation (5a) is $C=0$. For negative $k=-p^2$ equation (6b) yields

$$\frac{\dot{G}}{DG} = \frac{F''}{F} = -p^2 \quad (6c)$$

and from equation (6c) the two ordinary differential equations are:

$$F'' + p^2F = 0 \quad (7a)$$

$$\dot{G} + Dp^2G = 0 \quad (7b)$$

The functions

$$F(x) = A \cos px + B \sin px \quad (8a)$$

and

$$G(t) = \exp \{-Dp^2t\} \quad (8b)$$

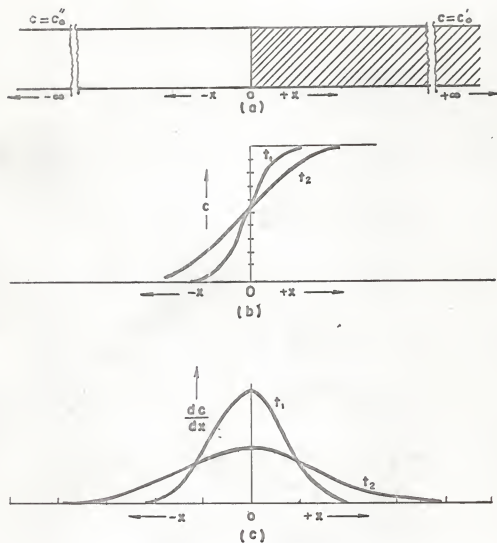


Fig. 1. Relation between concentration and distance of migration in diffusion cell. (a) Graphical representation of initial concentrations in the diffusion cell. $c_0' > c_0''$. (b) Relation between concentration and distance of migration given by equation (22). $t_2 > t_1$. (c) Relation between concentration gradient and distance of migration given by equation (23). $t_2 > t_1$.

are the solutions of equations (7a) and (7b) respectively, with A and B the arbitrary constants. Equation (6) can be rewritten as

$$c(x, t; p) = F(x)G(t) = (A \cos px + B \sin px) \exp \{-Dp^2 t\} \quad (9)$$

Equation (9) is the solution of equation (2). The constant of separation was chosen negative ($k = -p^2$) because positive values of k lead to an increasing exponential function in equation (9).

Any series of functions in equation (9) found in the usual manner by taking p as a multiple of fixed number, would lead to a function which is periodic in x when $t=0$. However, since $f(x)$ in equation (5a) is not assumed periodic, Fourier integrals should be used in this case instead of Fourier series. Since A and B are arbitrary constants in equation (9), they can be considered as functions of p as follows:

$$A = A(p) \quad (10a)$$

$$B = B(p) \quad (10b)$$

Since the diffusion equation (2) is linear and homogeneous, the function

$$c(x, t) = \int_0^{\infty} [A(p) \cos x + B(p) \sin x] [\exp \{-Dp^2 t\}] dp \quad (11)$$

is then the solution of equation (2) provided this integral exists and can be differentiated twice with respect to x and once with respect to t.

From equation (11) and the initial conditions given by equation (5a) it follows that

$$c(x, 0) = \int_0^{\infty} [A(p)\cos x + B(p)\sin x] dp \quad (12)$$

Introduction of a new variable of integration v in equation (12)

yields (9)

$$A(p) = \frac{1}{\pi} \int_{-\infty}^{\infty} f(v)\cos pvdv \quad (13)$$

$$B(p) = \frac{1}{\pi} \int_{-\infty}^{\infty} f(v)\sin pvdv \quad (13a)$$

The fourier integral given by equation (12) can be written as

$$c(x, 0) = \frac{1}{\pi} \int_0^{\infty} \int_{-\infty}^{\infty} f(v)\cos(px-pv)dv] dp \quad (14)$$

and equation (11) becomes

$$c(x, t) = \frac{1}{\pi} \int_0^{\infty} [f(v)\cos(px-pv) \exp(-Dp^2t)] dp \quad (15)$$

The integration of equation (15) yields (see Appendix for details)

$$c(x, t) = \frac{1}{2\sqrt{\pi Dt}} \left[\int_{-\infty}^{\infty} f(v) \exp\left\{-\frac{(x-v)^2}{4Dt}\right\} dv \right] \quad (16)$$

Equation (16) can be rewritten as

$$c(x, t) = \frac{1}{2\sqrt{\pi Dt}} \left[\int_{-\infty}^{\infty} f(v) \exp\left\{-\frac{(x-v)^2}{4Dt}\right\} dv + \int_0^{\infty} f(v) \exp\left\{-\frac{(x-v)^2}{4Dt}\right\} dv \right] \quad (17)$$

to take care of the two initial conditions given by equation (5a). In

equation (17) $f(v)=c''_0$ for the first integrand and $f(v)=c'_0$ for the

second integrand. With these values of $f(v)$ equation (17) can be

written as

$$c(x, t) = \frac{1}{2\sqrt{\pi Dt}} \left[c''_0 \int_{-\infty}^{\infty} \exp\left\{-\frac{(x-v)^2}{4Dt}\right\} dv + c'_0 \int_0^{\infty} \exp\left\{-\frac{(x-v)^2}{4Dt}\right\} dv \right] \quad (18)$$

If a new variable $\xi = \frac{(x-v)}{2\sqrt{Dt}}$ is introduced in equation (18), then equation (18) can be written as

$$c(x, t) = \frac{1}{\sqrt{\pi}} \left[c''_0 \int_{-\infty}^{\infty} \exp(-\xi^2) d\xi + c'_0 \int_0^{\infty} \exp(-\xi^2) d\xi \right] \quad (19a)$$

since $dv = -2\sqrt{Dt} d\xi$

Introduction of the error function according to the relation

$$\int_a^b \exp(-\xi^2) d\xi = \frac{\sqrt{\pi}}{2} (\operatorname{erfb} - \operatorname{erfa}) \quad (19b)$$

into equation (19a) yields

$$c(x, t) = \frac{1}{2} \left[c''_0 \left\{ \operatorname{erf} \frac{x}{2\sqrt{Dt}} - \operatorname{erf}(\infty) \right\} + c'_0 \left\{ \operatorname{erf}(-\infty) - \operatorname{erf} \frac{x}{2\sqrt{Dt}} \right\} \right] \quad (20)$$

Keeping in mind that $\operatorname{erf}(-x) = -\operatorname{erf}(x)$ and $\operatorname{erf} \infty = 1$, equation (20)

can be rewritten as

$$c(x, t) = \frac{1}{2} \left[c''_0 \left\{ \operatorname{erf} \frac{x}{2\sqrt{Dt}} - 1 \right\} + c'_0 \left\{ -1 - \operatorname{erf} \frac{x}{2\sqrt{Dt}} \right\} \right] \quad (21a)$$

Rearrangement of equation (21a) yields

$$c(x, t) = d'_0 - \frac{(c'_0 - c''_0)}{2} \left[1 - \operatorname{erf} \left(\frac{x}{2\sqrt{Dt}} \right) \right] \quad (22)$$

Equation (22) which is the solution of equation (2) can be shown to fulfill the conditions given by equations (5a) and (5b) (See Appendix II for details). The concentration distribution given by equation (22) is shown in Figure 1 (b).

Differentiation of equation (22) with respect to x yields

$$\frac{dc}{dx} = \frac{(c'0 - c''0)}{2 \sqrt{\pi Dt}} \exp\left(-\frac{x^2}{4Dt}\right) \quad (23)$$

(See Appendix III for details). The concentration gradient given by equation (23) is shown in Figure 1 (c).

MATERIALS AND METHOD

Materials

Sucrose (cane sugar) and water were the basic materials used in this study. Sucrose was used because it is available in high purity. Doubly distilled water was used to insure its purity. Two aqueous sucrose solutions of 0.10 g sucrose/ml of solution and 0.30 g sucrose/ml of solution were prepared by weighing accurately the required amounts of sucrose and then adding doubly distilled water making the total volume of 100. ml of solution. Dissolved air was not taken into consideration. The accuracy of the prepared solutions was checked by measuring the refractive indices with a Bausch & Lomb refractometer which was equipped with the international weight percent sucrose scale. The prepared solutions were found accurate within 0.4%.

Distilled water and acetone were used to wash the partially metallized slides used in forming the optical wedge diffusion cell. The acetone was used to remove the water marks left on drying the slides.

Method

The method used in this study is based on the determination of refractive index gradient by interferometric measurements. It was developed by Nishijima and Oster (2). The diffusion cell in this method consisted of an interferometric wedge which was, perhaps, the simplest of all the interferometric methods to adjust, and was easy to use for microscopic observation.

A parallel beam of monochromatic light transversing an optical wedge will interfere with that portion of light which is partially reflected (10). When the optical distance which is the product of the geometric distance Y and refractive index n of the medium in the wedge, is some odd integral number of half the wavelength λ of the light used, then there is cancellation, as shown in Figure 2 (a). If the refractive index n of the medium in the wedge is constant throughout the wedge, then the optical distance between two successive beams vary linearly along the length of the wedge, giving equally spaced interference fringes as shown in Figure 2 (b). The distance d between two successive fringes is given by the formula (10)

$$d = \lambda/2n\theta \quad (24)$$

where λ is the wavelength of the light used, n is the refractive index of the wedge medium, and θ is the wedge angle.

Now when some of the space in the wedge is replaced by a liquid of refractive index n , then the optical distance between two successive beams is greater by a factor n than that when air of refractive index 1.0 is the wedge medium. Hence, the fringes are closer together. In this case a discontinuous interface between the liquid-air system is obtained as shown in Figure 2 (c). On the other hand, when two diffusing liquids are placed in the wedge, then the refractive index across the interface varies continuously so that curved interference fringes are obtained. The interference pattern obtained for two diffusing liquids in the wedge shows a discontinuous interface similar to that in Figure 2 (c) at time $t=0$ when the boundary between the two liquids is formed. Figure 2 (d) shows the interference pattern obtained between the two diffusing liquids at any instant after the boundary is formed. The interference pattern of Figure 2 (d) has two important characteristics on which the experimental method depends:

- (1) Along any line drawn parallel to the original interface, the distance d between the two successive fringes is constant. In other words, along any fringe the optical distance which is the product of the geometric distance Y and refractive index n of the medium is constant, that is, the fringes represent contour lines of constant optical distance; and

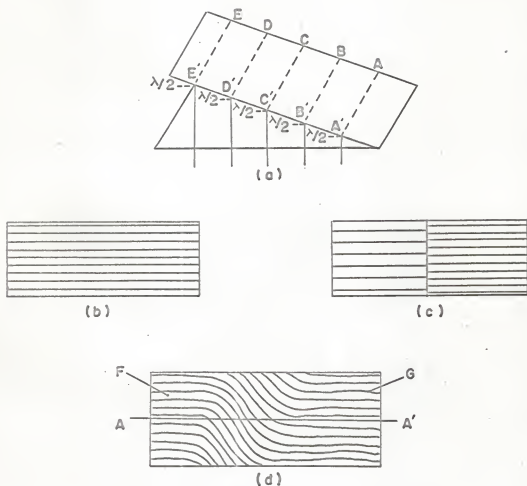


Fig. 2. The various interference patterns obtained by an optical wedge diffusion cell. (a) The cancellation of light beam according to equation (24). (b) The interference pattern obtained when air is the medium in the cell. (c) The discontinuous interface obtained with two non-diffusing liquids. (d) The interface pattern for two diffusing liquids at time $t > 0$. Note the continuous interface. A-A' is the reference line drawn parallel to the straight parallel fringes in the bulk of the two liquids denoted by F and G.

(2) Any line A-A' drawn perpendicular to the original interface, that is, drawn parallel to the fringes in the constant refractive index in the bulk of two liquids as shown in Figure 2 (d), represents a line of constant wedge thickness. The change of the optical path along this reference line A-A' depends only on the change in the refractive index along this line. If the refractive index along this line were constant then no fringe would have crossed it. The curved fringes are obtained only because the refractive index across the boundary varies continuously. Along the reference line A-A' the closer the fringes which cross the reference line, the greater the variation of the refractive index along this line. A plot of the density of fringes against distance along the reference line is a refractive index gradient curve.

Equation (23) can be rewritten in terms of refractive index gradient as follows:

$$\frac{dc}{dx} = \frac{(c'_{0}-c''_{0})}{2 \sqrt{\pi Dt}} \exp \left(-\frac{x^2}{4Dt} \right) \quad (23)$$

Since refractive index is assumed to be a linear function of the solute concentration, dn/dc is constant. Hence,

$$(c'_{0}-c''_{0}) = k(n_2-n_1) \quad (23a)$$

where n_2 and n_1 are the refractive indices corresponding to the solute concentration c'_{0} and c''_{0} respectively. The refractive index gradient can be written as

$$\frac{dn}{dx} = \frac{dn}{dc} \cdot \frac{dc}{dx} = \frac{1}{k} \frac{dc}{dx} \quad (23b)$$

where dc/dx is the concentration gradient and $dn/dc = 1/k$ is a constant. Substitution of equation (23a) into equation (23) and then the substitution of the resulting expression into equation (23b) yields

$$\frac{dn}{dx} = \frac{(n_2 - n_1)}{2 \sqrt{\pi Dt}} \exp \left(- \frac{x^2}{4Dt} \right) \quad (25a)$$

Equation (25a) is the relation between the refractive index gradient dn/dx and the distance x from the original boundary. This is true, provided the refractive index is a linear function of the solute concentration. In order to compare equation (25a) with a normal distribution the following substitution is made

$$\sigma = \sqrt{2Dt} \quad (25b)$$

Then equation (25a) yields

$$\frac{dn}{dx} = \frac{(n_2 - n_1)}{\sigma \sqrt{2\pi}} \exp \left(- \frac{x^2}{2\sigma^2} \right) \quad (26)$$

Equation (26) is the normal distribution equation of Gauss, where σ is the standard deviation. $(n_2 - n_1)$ will be the cumulative frequency.

σ can be determined by assuming the refractive index gradient curve to be normally distributed according to equation (26). Then the diffusion coefficient is calculated as follows:

$$D' = \sigma^2 / 2t' \quad (27)$$

The primed notation is used here because of the necessity of a zero time correction in the computation of the experimental diffusion coefficient. In equation (27) D' is the observed diffusion coefficient, t' is the observation time and σ as defined previously is the standard deviation of the normal or Gaussian distribution.

Apparatus

The optical wedge diffusion cell was placed on the stage of a microscope attached to the photomicrographic camera. A laser beam was used as the source of the monochromatic light. The basic components of the apparatus are shown in Figures 3 and 4. A brief discussion of the basic components of the apparatus used is given below:

(1) The Optical Wedge Diffusion Cell. Two 3" x 1" ordinary microscopic slides with one side partially metallized were used to form the optical wedge diffusion cell. These slides were made by the Tokyo Electronics Corps., Tokyo, Japan. Each slide was partially coated on one side so as to give about 85% reflectivity and 15% absorption of the incident light. One of these slides with its partially metallized surface upwards was placed on the microscope stage as shown in Figure 5 (a). One 7/8" x 7/8" coverslip of thickness 0.20 millimeter was placed on one end of this slide as shown in Figure 5 (b). The second slide with its partially metallized side downwards was placed over the coverslip to form a wedge as shown in Figure



Fig. 3. The microscope and camera used in this study. (A) Bausch and Lomb photomicrographic camera model L with Poloroid Land Back camera attachment. (B) Bausch and Lomb student series microscope. (C) Heating stage for accurate temperature control.

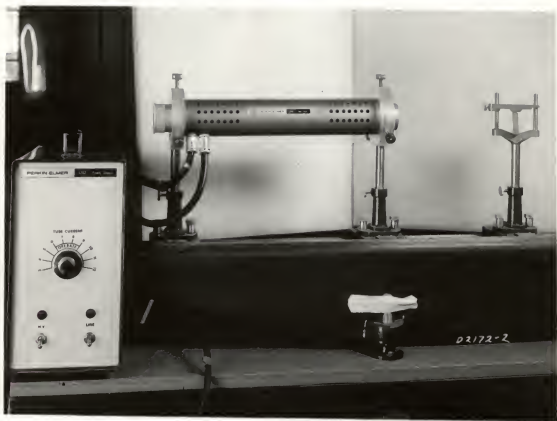


Fig.4. Perkin - Elmer Model 5200 Gas Laser used as the monochromatic light source in this study. The wavelength of the output light beam was 6328°A .

5 (c). The wedge thus formed was an optical wedge diffusion cell used for obtaining the interference fringes described previously.

(2). The Microscope and the Camera. A Bausch & Lomb Student series microscope with an objective lens of N.A. 0.09 and magnification power of 3.5 was used along with an ultraplane lens of magnification power 7.0 as an eyepiece. This ultraplane lens is a combination of high precision negative lenses in order to reduce the distortion of the image due to the curvation of the field.

The camera was Bausch & Lomb Photomicrographic camera Model L. It was mounted with Bausch & Lomb reflex attachment with Poloroid Land Back camera. The Poloroid attachment was very useful because the success or failure of the diffusion observation could be determined within a few minutes. A Poloroid black and white transparency film Type 46-L which is sensitive to the visible range of light was used. The exposure needed was about one second because of the low intensity of the light used. The transparencies were particularly useful during the measurements, since the microphotometer employed to measure the distances works in the density of the light. A brief description of the microphotometer is given in Appendix IV..

(3) Monochromatic Light Source. The monochromatic light source was a laser beam of wavelength 6328 \AA generated by a Perkin-Elmer Model 5200 Gas Laser. The laser is an acronym standing for light amplification by stimulated emission of radiation, and is highly

monochromatic by nature. As a result no elaborate optics to filter the wavelengths from the source is needed. Furthermore, it is very intense, coherent and narrow, thus eliminating the condensing lenses and other focusing optics to render the parallelism of the incident beam.

Experimental Method

The experimental procedure followed in each diffusion run was to micropipette 0.02 milliliter of each of the two sucrose solutions onto the partially metallized surface of one of the microscopic slides. The first slide was already in place on the microscope stage. The drops were placed side by side along the width of the slide as shown in Figure 5 (a). They should not touch each other. Then the second slide was placed over the first to form the optical wedge as shown in Figures 5 (b) and 5 (c). The two liquid drops were thus forced into physical contact as shown in Figure 5 (b). The stopwatch was started at the time the wedge was formed. The field under the microscope was selected in a region where the interface was perpendicular to the interference fringes. If such a region was not found then the slides were washed with water followed by acetone and the diffusion run was repeated. Extreme care was necessary so as not to disturb the angle of the wedge or its direction.

Four observations of each diffusion run were recorded by taking pictures at successive time intervals. The first observation was made



(a)



(b)



(c)

Fig. 5. The formation of the optical wedge diffusion cell. (a) First slide with its partially reflecting surface is placed on microscope stage. (b) The glass cover-slip is placed on the partially reflecting surface of the first slide. (c) The second slide with its partially reflecting surface downward is placed on the cover-slip to form the optical wedge diffusion cell.

after about sixty seconds to give time for the initial turbulence to die out. The last picture was taken before the diffusing interface had spread out of the photographic field.

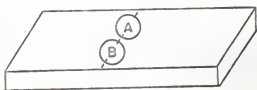
After each run, the partially reflecting slides were thoroughly washed with distilled water followed by acetone to remove the water marks on drying.

The temperature must be kept constant for different runs in order to deduce any comparable results. This was accomplished by selecting those hours of night when the temperature did not vary by more than 0.5°C . The night hours were also desirable to avoid any mechanical disturbances during the long exposure time for the type of film used.

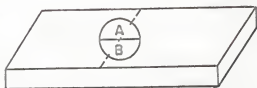
On the pictures taken, a reference line A-A' was drawn parallel to the straight parallel ends as shown in Figure 2(d). Then the distances between the fringes crossing the reference line were measured with the aid of microphotometer. These distances were reduced to the actual distances by dividing them with the magnification power of the microscope. From these measurements the refractive index gradient was calculated and plotted against x , the migration distance.

Calculation of Diffusion Coefficient

The curves obtained in the manner described previously are of the same nature as equation (23). The calculation of the diffusion coefficients is based on the assumption that in the ideal case the



(a)



(b)

Fig. 6 . The relative positions of the two diffusing liquids on the bottom slide of the optical wedge diffusion cell. (a) Before the upper slide of the cell is placed. The two drops dont touch each other. (b) After the upper slide is placed to form the optical wedge diffusion cell. The two liquids are thus forced into physical contact.

curves have the properties of the Gaussian distribution curves (11). The symbols which are commonly used in calculating the diffusion coefficient and their definitions are illustrated in Figure 7.

The statistical method developed by Pearson and applied to the present problem by Lamm is outlined by Neurath (11). It consists of treating the experimental curves as ideal distribution curves. The standard deviation σ is given by

$$\sigma = \sqrt{\mu^0_2} \quad (28)$$

where μ^0_2 is the second moment of the curve about the centroidal axis. The centroidal axis is that axis about which the first moment is zero. The observed diffusion coefficient D' is related to σ by

$$D' = \sigma^2 / dt' \quad (27)$$

where t' is the time of diffusion. In practice, the base line of the diffusion curve or the refractive gradient curve is divided into evenly spaced unit breadth, numbered outward from an arbitrarily chosen origin near the center of the base-line. If s_i is the respective number on the base-line and S_i the corresponding ordinate then the zero moment of the curve about the arbitrarily chosen origin is

$$\mu'_0 = \Sigma S_i = N \quad (29a)$$

where N is the cumulative frequency. μ'_1 , the first moment about this axis is

$$\mu'_1 = \frac{\sum S_i s_i}{N} \quad (29b)$$

The second moment μ'_2 about the arbitrary centroidal axis is

$$\mu'_2 = \frac{\sum S_i s_i^2}{N} \quad (29c)$$

The true position of the centroidal axis is

$$x_0 = s_0 - \mu'_1 \quad (29d)$$

and the true second moment μ_2 about the centroidal axis is

$$\mu_2 = \mu'_2 - (\mu'_1)^2 \quad (29e)$$

The second moment calculated in this manner has yet to be transferred into absolute units by the relation

$$\mu^o_2 = \mu_2 w^2 \quad (30)$$

where w is the arbitrary distance between the successive chords S .

The extent to which the experimental curve deviates from the ideal or computed curve can be studied by plotting the computed curve by the use of the Z column in Sheppard's table in the Tables for Statisticians and Biometricians (12).

In this study, the third and fourth moments about the centroidal axis along with the statistics β_1 , β_2 and k were computed to check the presence of skewness as suggested by Elderton (13). The following equations were used in these calculations:

The third moment μ'_3 about the arbitrary centroidal axis is

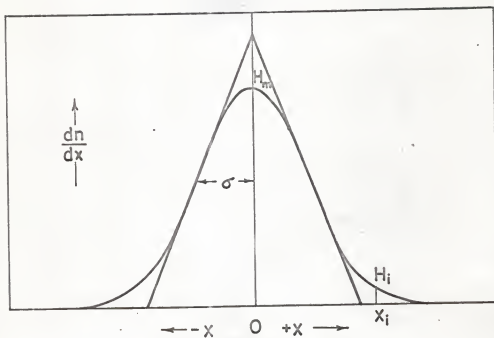


Fig. 7. Refractive index gradient curve illustrating the symbols and their meanings used in calculating diffusion coefficient. H_m is the maximum ordinate at $x=0$; σ is the standard deviation; H_i is the ordinate corresponding to x_i on the abscissa. The relation between standard deviation σ , the observation time t' , and the observed diffusion coefficient D' is given by equation (27).

$$\mu'_3 = \frac{\sum S_i s_i^3}{N} \quad (31a)$$

and the true third moment about the centroidal axis is

$$\mu_3 = \mu'_3 - 3\mu'_1\mu'_2 + 2(\mu'_1)^3 \quad (31b)$$

The third moment must also be transferred to absolute units by the relation.

$$\mu^0_3 = \mu_3 w^3 \quad (31c)$$

Similarly, the fourth moment μ'_4 about the arbitrary centroidal axis is

$$\mu'_4 = \frac{\sum S_i s_i^4}{N} \quad (32a)$$

and the true fourth moment about the centroidal axis is

$$\mu_4 = \mu'_4 - 4\mu'_1\mu'_3 + 6(\mu'_1)^2\mu'_2 - 3(\mu'_1)^4 \quad (32b)$$

The fourth moment is also transferred into absolute units by the relation

$$\mu^0_4 = \mu_4 w^4 \quad (32c)$$

The statistical β_1 is given by the relation

$$\beta_1 = (\mu^0_3)^2 / (\mu^0_2)^3 \quad (33)$$

and for the normal curve it must be zero (13).

The statistical β_2 is given by the relation

$$\beta_2 = (\mu^0_4) / (\mu^0_2)^2 \quad (34)$$

and for the normal curve it must be three (13).

The statistics k is given by the relation

$$k = \beta_1(\beta_2+3)/4(4\beta_2-3\beta_1)(2\beta_2-3\beta_1-6) \quad (35)$$

and for the normal curve it must be zero (13).

The sample data along with the sample calculations are given in Appendix VI. A ForGo program to evaluate the moments and statistics on an IBM 1620 computer is presented in Appendix V.

The Zero-time Correction of Observation Time t'

When the two liquids are brought into physical contact by lowering the upper slide of the optical wedge diffusion cell, there would be some initial mixing of the two liquids. This initial mixing causes the concentration distribution at any time to appear as though the boundary has been formed before this actually happened. The time between the apparent and actual boundary formation must be calculated and added to the observation time t' . This extrapolation of t' to the zero-time, the time when the boundary was apparently formed, is called the zero-time correction. The plot of the observed diffusion coefficient D' against the reciprocal of the observation time t' yields a straight-line as shown by Longworth (14).

D'_0 the value of the diffusion coefficient corrected for zero-time is given by the relation (14)

$$D'_0 = \sigma^2/2(t'+\Delta t) \quad (36)$$

where σ is the calculated standard deviation, t' is the observation

time and Δt is the increment which must be added to t' in order to take care of the initial mixing of the two diffusing liquids. This Δt can be evaluated from the linear relation between D' and $1/t'$. The rearrangement of equation (36) yields

$$2D'_0(t'+\Delta t) = \sigma^2 \quad (37a)$$

Dividing equation (37a) by $2t'$ yields

$$D'_0 + \frac{D'_0 \Delta t}{t'} = \sigma^2 / 2t' \quad (37b)$$

But the right hand side of equation (37b) is equal to D' , the observed diffusion coefficient by equation (27). Hence equation (37b) can be rewritten as

$$D'_0 + \frac{D'_0 \Delta t}{t'} = D' \quad (37c)$$

The rearrangement of equation (37c) yields

$$D' = D'_0 \left(1 + \frac{\Delta t}{t'}\right) \quad (38)$$

Equation (38) can be written as

$$D' = a + \frac{m}{t'} \quad (39)$$

where $a=D'_0$ is the intercept and $m=D'_0 \Delta t$ is the slope of the straight line obtained from the plot of D' vs $1/t'$. Δt can be evaluated from the slope and intercept of the straight line on the plot of D' vs $1/t'$.

By comparing equation (39) with equation (38) one obtains

$$\Delta t = \frac{m}{a} \quad (40)$$

where m and a are defined by equation (39).

RESULTS AND DISCUSSION

Experimental investigations were carried out to obtain the diffusion coefficient for the system consisting of $\Delta c = c_2 - c_1 = 0.20$ g sucrose/ml of solution and $c_{avg} = (c_2 + c_1)/2 = 0.20$ g sucrose/ml of solution. The calculations were made for two diffusion runs, each consisting of four observations by the method outlined previously.

The experimental refractive index gradient curve along with the curves computed according to equation (26) for diffusion Runs 1 and 2 are given in Figures 8 through 11 and Figures 12 through 15 respectively. From these figures it can be seen that the experimental curves deviate only slightly from the computed curves in the intermediate range of x , the distance of migration. The deviation of the experimental curve from the computed curve can be attributed partially to the difference in standard deviations, in addition to the experimental errors. Since the range of dn/dx does not start near zero, the area used in the computation of σ was less than the actual area under the curve. As a result the value of the standard deviation varied between 88% and 96% of the actual value of standard deviation. However, there was no correction technique available which could be applied; hence, the computation of σ was carried out on the basis of 100% area under the curve. The difference between the computed and the actual σ 's becomes apparent farther away from the centroidal axis, signifying that the computed σ is smaller than the actual σ .

The diffusion time or observation time t' , the computed standard deviation σ , and the observed diffusion coefficient D' for each observation in diffusion runs 1 and 2 are presented in Tables 1 and 2 respectively.

The plots of D' vs $1/t'$ for diffusion runs 1 and 2 are presented in Figure 16. The equation of the straight line for Run 1 is

$$D' = 3.4032 \times 10^{-4} + \frac{B.2357 \times 10^{-4}}{t'} \text{ mm}^2/\text{second} \quad (41)$$

Comparison of equation (41) with equations (39) and (40) yields $t=242$ seconds and $D'_0 = 3.4032 \times 10^{-4}$ square millimeters/seconds for Run 1. The values D'_0 , the zero-time corrected diffusion coefficients computed by equation (36), the observation time t' , and the percent deviation of D'_0 from the mean value of D'_0 for each observation in Run 1 are presented in Table 3. The mean value of $D'_0 = 3.3946 \times 10^{-4}$ $\text{mm}^2/\text{second}$ which is the arithmetic mean value of the four zero-time corrected D'_0 , is henceforth, taken as the experimental diffusion coefficient D for the comparison with the predicted diffusion coefficient for the average concentration of 0.20 g sucrose/ml of solution.

The equation of the straight line for Run 2 in Figure 16 is

$$D' = \left[3.2062 \times 10^{-4} + \frac{1.2744 \times 10^{-1}}{t'} \right] \text{ mm}^2/\text{second} \quad (42)$$

Comparison of equation (42) with equations (39) and (40) yields

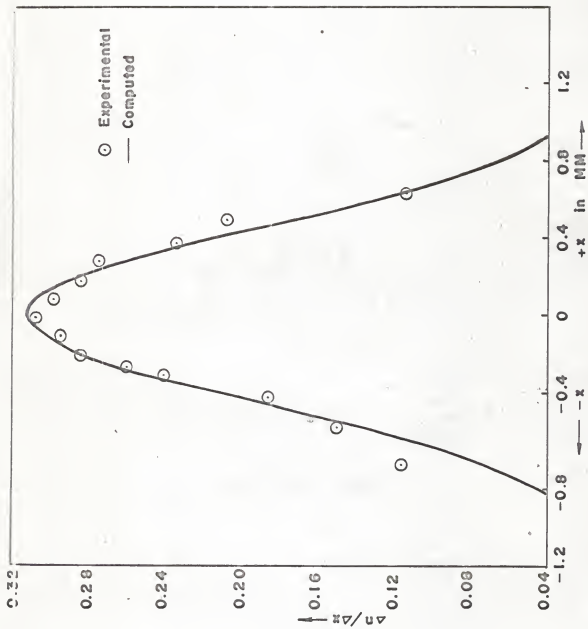


Fig. 8. Refractive index gradient curve. System: $\Delta c = 0.2$ g sucrose /ml. solution. $C_{avg} = 0.2$ g sucrose/ml. solution. Observation time = 64 seconds. Run 1.

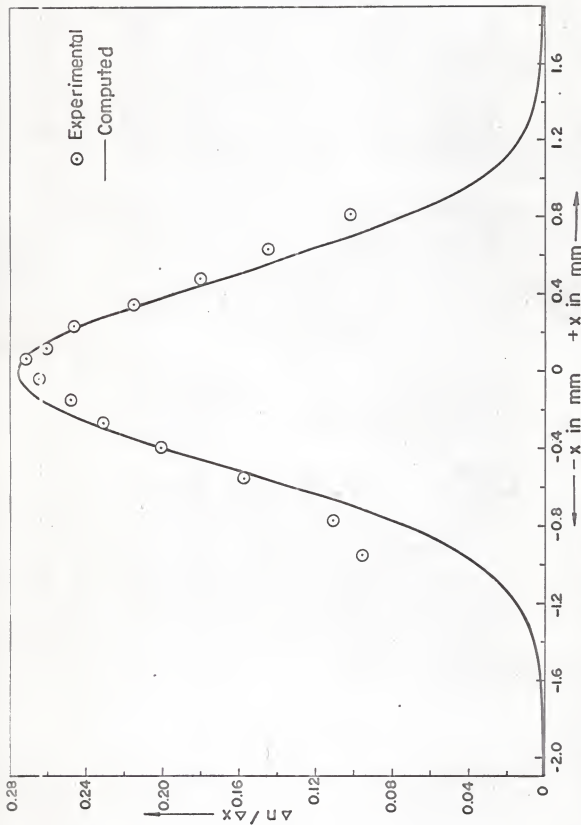


Fig. 9. Refractive index gradient curve. System: $\Delta c = 0.2$ g. sucrose/ml. soln.
 $c_{\text{avg}} = 0.2$ g. sucrose/ml. soln. Observation time = 104 seconds. Run 1.

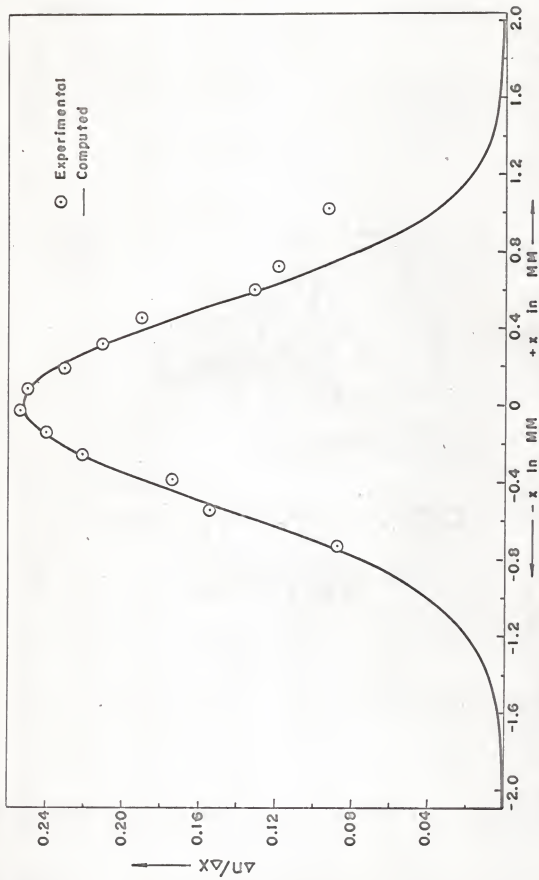


Fig. 10. Refractive index gradient curve. System: $\Delta c=0.2$ g. sucrose/ml. solution, $c_{\text{avg.}}=0.2$ g. sucrose/ml. solution. Observation time = 154 seconds, Run 1.

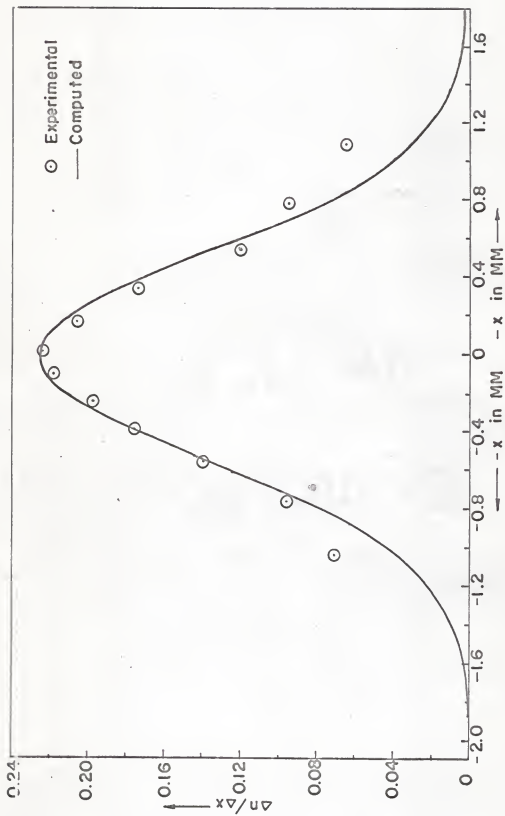


Fig. 11. Refractive index gradient curve. System: $\Delta c = 0.2$ g sucrose / ml. solution. $c_{avg} = 0.2$ g sucrose / ml. solution. Observation time = 214 seconds. Run 1.

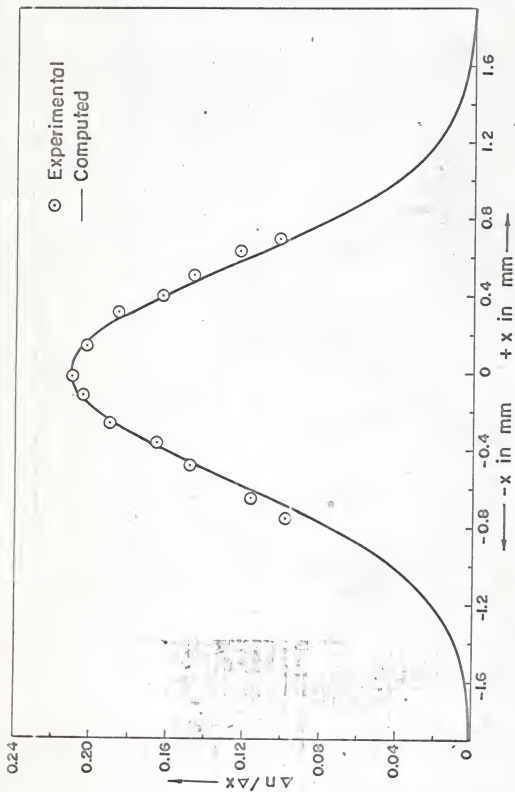


Fig. 12. The refractive index gradient curve. System: $\Delta c = 0.2$ g. sucrose/ml. solution, $c_{\text{avg}} = 0.2$ g. sucrose/ml. solution. Observation time 74 seconds. Run 2.

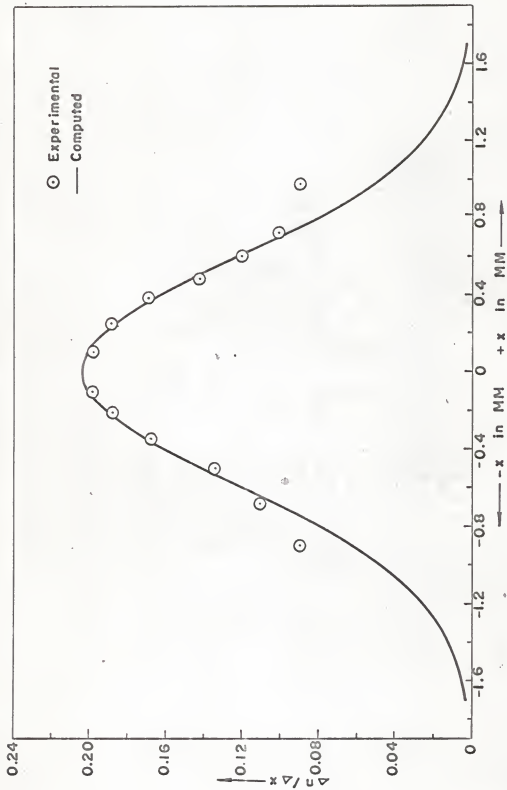


Fig. 13. The refractive index gradient curve. System: $\Delta c = 0.2$ g sucrose / ml. solution, $C_{\text{avg.}} = 0.2$ g sucrose / ml. solution. Observation time = 124 seconds Run 2.

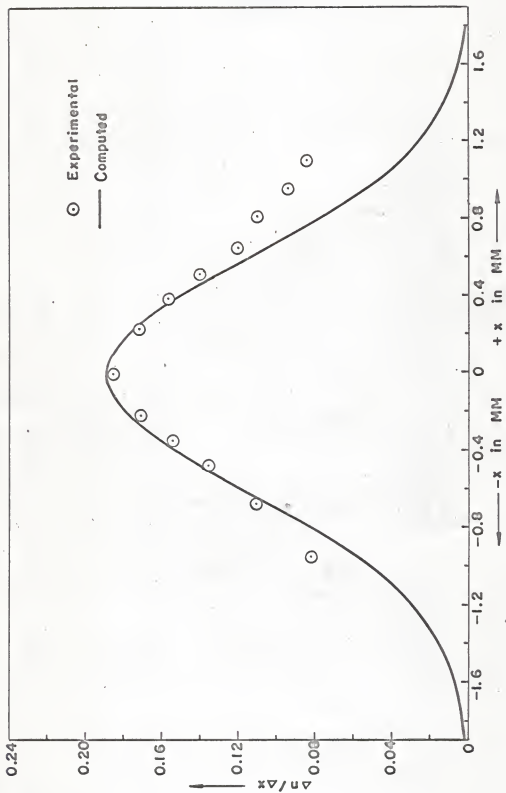


Fig. 14. The refractive index gradient curve. System: $\Delta c = 0.2$ g. sucrose / ml. solution, $c_{\text{avg.}} = 0.2$ g sucrose / ml. solution. Observation time = 184 seconds. Run 2.

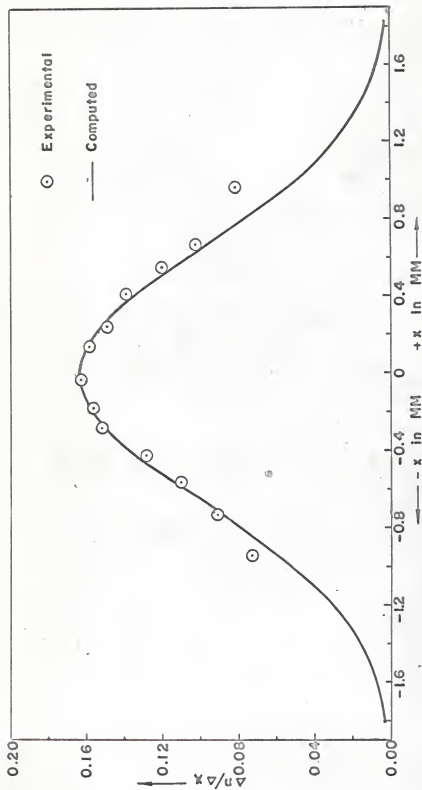


Fig.15. The refractive index gradient curve. System: $\Delta c = 0.2$ g. sucrose/ml. solution, $C_{avg.} = 0.2$ g sucrose/ml solution. Observation time = 244 seconds. Run 2.

Table 1. Tabulation of diffusion coefficient D' computed from equation (27) for Run 1. System: $\Delta c = 0.20$ g sucrose/ml of solution, $c_{avg} = 0.20$ g sucrose/ml of solution. Temperature 25°C .

Observation time t' in seconds	Calculated standard deviation σ	Diffusion coefficient $D' \times 10^4 \text{ mm}^2/\text{second}$
64.0	0.45604	16.2480
104.0	0.49012	11.5490
154.0	0.51745	8.6923
214.0	0.55021	7.0730

Table 2. Tabulation of diffusion coefficient D' computed from equation (27) for Run 2. System: $\Delta c = 0.20$ g sucrose/ml of solution, $c_{avg} = 0.20$ g sucrose/ml of solution. Temperature: 24.7°C .

Observation time t' in seconds	Calculated standard deviation σ	Diffusion coefficient $\times 10^4 \text{ mm}^2/\text{second}$
74.0	0.54881	20.3510
124.0	0.58396	13.7500
184.0	0.60552	9.9635
244.0	0.64517	8.5440

$\Delta t = 397$ seconds and $D'_0 = 3.2062 \times 10^{-4}$ mm²/second for Run 2.

The values of D'_0 computed by means of equation (36), the observation time t' , and percent deviation of D'_0 from the mean value of D'_0 for each observation in Run 2 are presented in Table 4. The mean value of $D'_0 = 3.2195 \times 10^{-4}$ mm²/second which is the arithmetic mean of the four zero-time corrected D'_0 in Run 2 has yet to be corrected for the temperature difference in the two runs.

For a small temperature difference the semi-empirical relation of Wilke and Chang (15) can be applied to the diffusion data.

According to Wilke and Change (15)

$$D = 7.4 \times 10^{-8} \frac{(\psi M_B)^{0.5} T}{\mu V_A^{0.6}} \quad (43a)$$

where V_A is the molar volume of the solute A in cm³/g-mole as liquid at its normal boiling point, μ is the viscosity of the solution in centipoises, ψ is an "association parameter" for the solvent B, M_B is the molecular weight of the solvent B, and T is the absolute temperature in °K. If D_2 and D_1 are two diffusion coefficients of the same system at temperatures T_2 and T_1 respectively, then D_2 and D_1 are related to each other by the following relation derived from equation (43a)

$$\frac{D_1 \mu_1}{T_1} = \frac{D_2 \mu_2}{T_2} \quad (43b)$$

The viscosity data for the sucrose solution are given in the Handbook of Physics and Chemistry (5). Substituting D_2 as the diffusion coefficient at $T_2 = 298 \text{ }^\circ\text{K}$, $\mu_1 = 1.695 \text{ cps}$, and $D_1 = 3.2195 \times 10^{-4} \text{ mm}^2/\text{sec}$. at $T_1 = 297.7 \text{ }^\circ\text{K}$ with $\mu_1 = 1.708 \text{ cps}$ in equation (43) and solving for D_2 yields

$$D_2 = 3.2411 \times 10^{-4} \text{ mm}^2/\text{second} \quad (43c)$$

This temperature corrected value of $D'_0 = 3.2411 \times 10^{-4} \text{ mm}^2/\text{second}$ is taken as the experimental value of the diffusion coefficient D of Run 2 for comparison with the predicted literature value of diffusion data for the average concentration of 0.20 g sucrose/ml of solution.

The zero-time correction Δt for Run 1 is 242 seconds while for Run 2 it is 397 seconds. The correction time was relatively large when compared to the observation time t' . This was due to the small volume of the system. Only 0.02 ml of each solution was used in the diffusion run. The initial mixing was caused when the upper partially reflecting slide of the optical wedge diffusion cell was placed. It was of such a large magnitude that it appeared as if the boundary had been formed long before it actually happened. There was also a marked difference in the two zero-time corrections. This can be attributed to the different degrees of initial mixing in the two runs. It seemed as if the initial mixing depended upon the original distance between the two droplets, and this distance could not be kept constant from run to run.

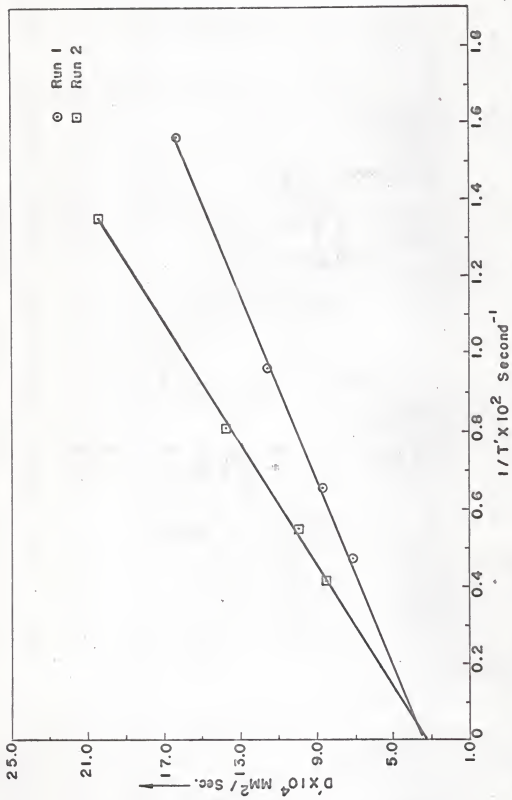


Fig.16: Application of equation (36) for zero-time correction to observed diffusion coefficient. System: $C_{avg} = 0.2$ g sucrose/ml. solution.

Table 3. Application of equation (36) to the observed diffusion data D' of Run 1. $\Delta t = 242$ seconds from equation (41).

Observation time t' in seconds	Observed diffusion coefficient $D' \times 10^4 \text{ mm}^2/\text{sec.}$	Corrected diffusion coefficient $D'_0 \times 10^4 \text{ mm}^2/\text{sec.}$	% deviation of D'_0 from mean D'_0
64.0	16.2480	3.3984	0.111
104.0	11.5490	3.4710	2.253
154.0	8.6923	3.3819	0.079
214.0	7.0730	3.3270	1.198
Mean $D'_0 = 3.3946$			

Table 4. Application of equation (36) to the observed diffusion data D' of Run 2. $\Delta t = 397$ seconds from equation (42).

Observation time t' in seconds	Observed diffusion coefficient $D' \times 10^4 \text{ mm}^2/\text{sec.}$	Corrected diffusion coefficient $D'_0 \times 10^4 \text{ mm}^2/\text{sec.}$	% deviation of D'_0 from mean D'_0
74.0	20.3510	3.1974	0.687
124.0	13.7500	3.2729	1.660
184.0	9.9635	3.1554	1.450
244.0	8.5440	3.2523	1.010
Mean $D'_0 = 3.2195$			

The experimental values of the diffusion coefficient D were compared with the values of D at an average concentration of 0.20 g sucrose/ml of solution predicted by the linear extrapolation of the data of Goesting and Morris (3) in the dilute concentration range of sucrose solution and of English and Dole (4) in the supersaturated concentration range of sucrose solution.

A straight line drawn by the least-square fit through the diffusion data of Goesting and Morris for the dilute sucrose concentration range is presented in Figure 17. The equation of this straight line is

$$D_{G-M} = D^0 + m c_{avg}$$

or

$$D_{G-M} = [5.2257 - 3.6787 C_{avg}] \times 10^{-4} \text{ mm}^2/\text{second} \quad (44)$$

where c_{avg} is in g sucrose/ml of solution. The same treatment to the diffusion data of English and Dole (4) for the saturated sucrose range yielded the following relation

$$D_{E-D} = [3.5909 - 3.1996 c_{avg}] \times 10^{-4} \text{ mm}^2/\text{second} \quad (45)$$

The predicted value of the diffusion coefficient D for the average concentration of 0.20 g sucrose/ml of solution based on Goesting-Morris' data is $3.6787 \times 10^{-4} \text{ mm}^2/\text{second}$, while that based on English-Dole's data is $2.9510 \times 10^{-4} \text{ mm}^2/\text{second}$

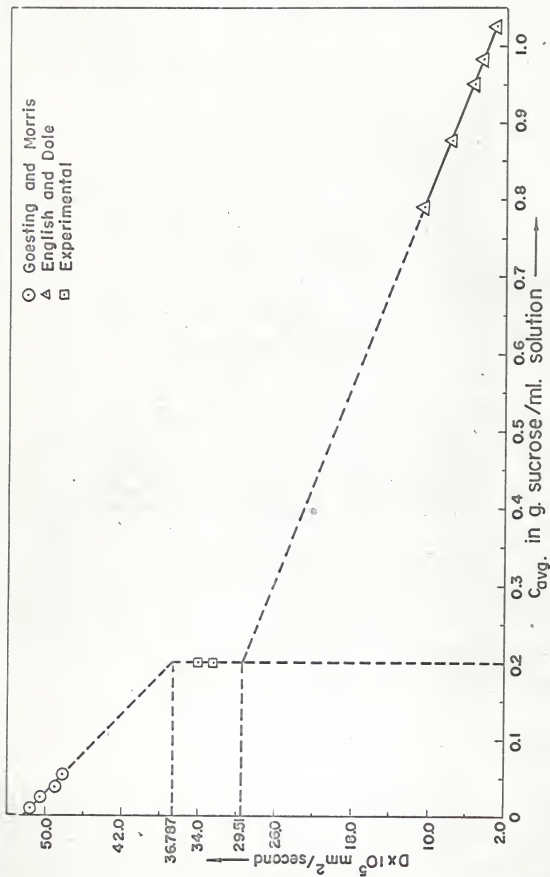


Fig. 17. Extrapolation of available literature data in dilute and concentrated range of aqueous sucrose solution.

calculated by means of equations (44) and (45) respectively. Comparison of the two experimental D with these predicted values is given in Table 5. The two experimental values of the diffusion coefficient D are in between the two predicted values of D based on the literature data in the two extreme ranges of sucrose concentration. The equations of straight line in the two concentration ranges have different slopes and intercepts compare equation (44) with equation (45) . Taking the above arguments into consideration, it can be suggested that the concentration dependence of the diffusion coefficient of the aqueous sucrose solution may be curvilinear instead of linear in the intermediate range of sucrose concentration.

Table 5. Comparison of the experimental diffusion coefficient D_{exp} with the predicted D based on the available literature diffusion data. System: $c_{\text{avg}} = 0.20$ g sucrose/ml solution. Temperature: 25 °C. All diffusion coefficients are in 10^{-4} mm²/second.

		% devi. of D_{exp} from predicted D based on data of	
Run No. :	Experimental diffusion coefficient D_{exp}	Goesting-Morris $D_{G-M} = 3.6787$	English-Dole $D_{E-D} = 2.9510$
1	3.3946	- 7.50	+15.35
2	3.2411	-12.22	+10.10

CONCLUSIONS

The set-up of the equipment for the adaptation of the technique of Nishijima and Oster (2) was satisfactory for the measurements of the diffusion coefficients of a binary liquid system.

According to the theory of Brownian movement, the average of the square of the distance over which a molecule moves is proportional to the time during which it travels. Therefore, if the diffusion is observed over a small distance, the time required for the observation can be reduced by the square of the magnification power. The optical wedge diffusion cell in this study was best suited for microscopic observations. The time required for the observation using this set-up was less than three hundred seconds for the diffusion study of sucrose solutions. When compared with the observation time in the conventional apparatus employed by other investigators for the same system, the observation time required in this set-up was, indeed, very small. The time of observation in the Gouy interferometer employed by Goesting and Morris in their study was between 4,000 and 40,000 seconds, while that in the Schlieren method employed by English and Dole in their studies of sucrose diffusion was between 5,000 and 30,000 seconds.

Another advantage of the technique used in this study was the requirement of a very small amount of each solution; only 0.02 ml of each of the two solutions was required in the diffusion run.

In the techniques used by Goesting and Morris as well as by English and Dole, at least 75 ml of each solution had to be drawn in each run. Because of the small amount of each solution in this study, no elaborate equipment for maintaining constant temperature was required. Only the room temperature control was required to insure that both the solutions were at the same temperature from run to run. However, a cooling stage on the microscope was fitted for very accurate temperature control after the data for this study were taken. With this added temperature control device, the need for the semi-empirical relation of Wilke and Chang, (15) to correct for a temperature difference from run to run, would be eliminated. This should prove very useful, especially for the systems for which no viscosity data are available.

The major change in this study from the conventional apparatus was the use of a laser beam as a source of monochromatic light in obtaining the interference fringe pattern of the two diffusing liquids. Because of the high purity of the light and the compactness of the laser, this change was very satisfactory. It eliminated the filtering and focusing optics needed in the conventional monochromatic light source. Furthermore, the operation of obtaining the monochromatic light was very simple; only a flip of a switch was needed.

The relatively large magnitude of the zero-time correction, t_0 , was due to the large magnitude of initial mixing of the two

diffusing liquids and to the very small volume of the system. Furthermore, the zero-time corrections for different runs were different because the original distances between two liquid droplets were different from run to run.

The experimental values of the diffusion coefficient D in two different runs for the system consisting of $\Delta c = 0.20$ g sucrose/ml solution and $c_{avg} = 0.20$ g sucrose/ml solution agreed with each other within 5%. The comparison of the experimental values of the diffusion coefficient obtained in this study with the predicted values of D based on the available literature data in the dilute and saturated ranges of aqueous sucrose solution suggests that the concentration-dependence of the diffusion coefficient in the sucrose-water system may be curvilinear instead of linear in the intermediate sucrose concentration range. However, further study should be conducted at various sucrose concentrations in the intermediate range for the confirmation of the nature of the concentration-dependence of D in this range.

RECOMMENDATIONS

Further study in this field should be directed toward a reasonably complete diffusion study of the intermediate sucrose concentration range, thus enabling us to establish the concentration-dependence of the diffusion coefficient in this range of concentration.

The following experimental hints may be useful in future work to be carried out with this equipment:

(1) The field of view can be increased or decreased by varying the magnification power of the microscope. It should be adjusted to give a maximum number of fringes crossing the reference line.

(2) The concentration difference and the thickness of the optical wedge diffusion cell should be selected to give the field of observation complete with the two straight parallel fringe ends. However, the thickness should not be so small that it obstructs the molecular motion. Large concentration differences between the two diffusing liquids should be avoided if possible, since this might lead to a skewed refractive index gradient curve (11). The need for the inclusion of the two straight and parallel ends in the pictures becomes very apparent when the refractive index gradient curve is skewed or asymmetric about the centroidal axis because the concentration-dependence of the diffusion coefficient can be obtained from the skewness by taking the higher moments about the centroidal axis of the refractive index gradient curve (16).

ACKNOWLEDGMENTS

The author wishes to express his sincere appreciation to Dr. L. T. Fan for his advice and guidance in this study. The author is also grateful to Mr. Frederick S. Jerome for his guidance and help in designing of the equipment as well as in the later part of this investigation.

Acknowledgment is given to Dr. Basil Curnutte, Jr., Professor in the Physics Department, whose cooperation and guidance made the use of the microphotometer possible. Acknowledgment is also given to Dr. Kali S. Banerjee, Professor in the Statistics Department, whose guidance in the statistical aspect of this investigation helped in this work.

The funds for this project were provided by the National Science Foundation project NSF GK67.

PARTIAL LIST OF SYMBOLS USED

- D' = Observed diffusion coefficient calculated from equation (
- D'_0 = Zero-time corrected diffusion coefficient calculated from equation (
- Mean D'_0 = Arithmetic mean of zero-time corrected diffusion coefficients in a given experimental run.
- D_{exp} = Value of Mean D' after the necessary temperature correction, taken as the experimental diffusion coefficient of a given experimental run.
- $D_{\text{G-M}}$ = Value of the diffusion coefficient predicted by the linear extrapolation of the data of Goesting and Morris in the extremely dilute sucrose concentration range.
- $D_{\text{E-D}}$ = Value of the diffusion coefficient predicted by the linear extrapolation of the data of English and Dole in the super-saturated sucrose concentration range.
- t' = Observed diffusion time in seconds.
- Δt = Zero-time correction of the observed diffusion time t' , in seconds.
- n = Refractive index of the sucrose solution.
- Δc = The difference in the sucrose concentration of the two diffusing sucrose solutions.

c_{avg} = The average concentration of the two diffusing sucrose solutions.

LITERATURE CITED

1. Touloukin, Y. C., "Retrieval Guide to Thermophysical Properties Research Literature," McGraw-Hill Book Co., New York, New York (1960).
2. Nishijima, Y., and G. Oster, *Journal of Chemical Education*, 38, 144 (1961).
3. Goesting, L. J., and M. S. Morris, *Journal American Chemical Society*, 71, 1998 (1949).
4. English, A. C., and J. Dole, *Journal American Chemical Society*, 72, 3261 (1950).
5. "Handbook of Physics and Chemistry," Student 4 Ed., Chemical Rubber Co. Publication, Cleveland, Ohio (1963).
6. Johnson, P. A., and A. L. Babb, *Chemical Reviews*, 56, 387 (1956).
7. Jost, W., "Diffusion in Solids, Liquids and Gases," Academic Press, Inc., New York, New York (1952).
8. Crank, J., "The Mathematics of Diffusion," Oxford University Press, Oxford, England (1956).
9. Kreyszig, E., "Advanced Engineering Mathematics," John Wiley and Sons, Inc., New York, New York (1964).
10. Tolansky, S., "Introduction to Interferometry," Longmans, Green and Co., Inc., London, England (1955).
11. Neurath, H., *Chemical Reviews*, 30, 357 (1942).
12. Pearson, K., "Tables for Statisticians and Biometricians Part I," Cambridge University Press, Cambridge, England (1903).
13. Elderton, W. P., "Frequency Curves and Correlation," Harren Press, Washington, D. C. (1953).
14. Longworth, W. P., *Journal American Chemical Society*, 69, 2521 (1947).

15. Wilke, C. R., and P. Chang, Am. Inst. Chem. Eng., 1, 264 (1955).
16. Nishijima, Y., and G. Oster, Journal of Chemical Physics, 27, 269 (1957).

APPENDIX I

Integration of equation (15).

Equation (15) can be integrated as follows:

$$c(x, t) = \frac{1}{\pi} \int_0^{\infty} \left[\int_{-\infty}^{\infty} f(v) \cos(px-pv) \exp(-Dp^2t) dv \right] dp \quad (15)$$

Assuming that the order of the integration may be inverted, equation (15) can be rewritten as

$$c(x, t) = \frac{1}{\pi} \int_{-\infty}^{\infty} \left[\int_0^{\infty} f(v) \cos(px-pv) \exp(-Dp^2t) dp \right] dv \quad (15a)$$

The inner integral can be evaluated by the use of the formula given in the Handbook of Physics and Chemistry (5)

$$\int_0^{\infty} \{ \exp(-s^2) \cos 2bs \} ds = \frac{\sqrt{\pi}}{2} e^{-b^2} \quad (15b)$$

Introduction of a new variable of integration by setting $s = \sqrt{Dt}$ and

$b = x-v/2\sqrt{Dt}$ equation (15b) yields

$$\int_0^{\infty} \{ \exp(-Dp^2t) \cos(px-pv) \} dp = \frac{\sqrt{\pi}}{2\sqrt{Dt}} \exp\left(-\frac{(x-v)^2}{4Dt}\right) \quad (15c)$$

Insertion of the result given by equation (15c) into equation (15)

yields

$$c(x, t) = \frac{1}{2 \sqrt{\pi Dt}} \left[\int_{-\infty}^{\infty} f(v) \exp \left(-\frac{(x-v)^2}{4Dt} \right) dv \right] \quad (16)$$

Equation (16) is the required expression.

APPENDIX II

Solution of Fick's second law satisfying the initial conditions

Equation (22) which is a solution of equation (2) fulfills the conditions given by equations (5a) and (5b) as follows:

$$c(x, t) = c'_0 - \frac{(c'_0 - c''_0)}{2} \left[1 - \operatorname{erf} \left(\frac{x}{2 \sqrt{Dt}} \right) \right] \quad (22)$$

Substituting the condition $x > 0$ given by equation (5a) into equation (22) yields

$$\begin{aligned} c(+x, 0) &= c'_0 - \frac{c'_0 - c''_0}{2} \left[1 - \operatorname{erf} \left(\frac{x}{0} \right) \right] \\ &= c'_0 - \frac{c'_0 - c''_0}{2} \left[1 - \operatorname{erf} (\infty) \right] \\ &= c'_0 - \frac{c'_0 - c''_0}{2} [1 - 1] \\ &= c'_0 \end{aligned}$$

Substituting the condition $x < 0$ given by equation (5a) into equation (22) yields

$$\begin{aligned} c(-x, 0) &= c'_0 - \frac{c'_0 - c''_0}{2} \left[1 - \operatorname{erf} \frac{-x}{D} \right] \\ &= c'_0 - \frac{c'_0 - c''_0}{2} [1 - (-1)] \end{aligned}$$

$$\begin{aligned} &= c'_0 - \frac{c'_0 - c''_0}{2} (2) = c'_0 - c'_0 + c''_0 \\ &= c''_0 \end{aligned}$$

Similarly, it can be shown that equation (22) fulfills the boundary conditions given by equation (5b), thus yields c'_0 or c''_0 depending on the sign of x .

APPENDIX III

Differentiation of equation (22) with respect to x

Equation (22) can be differentiated with respect to x as follows:

$$c(x, t) = c'_0 - \frac{c''_0 - c''_1}{2} \left[1 - \operatorname{erf} \left(\frac{x}{2 \sqrt{Dt}} \right) \right] \quad (22)$$

Substituting $\xi = x/2\sqrt{Dt}$ into equation (23) yields

$$c(x, t) = c'_0 - \frac{c''_0 - c''_1}{2} \left[1 - \operatorname{erf}(\xi) \right] \quad (22a)$$

Now $\operatorname{erf}(\xi)$ is the notation for

$$\operatorname{erf}(\xi) = \frac{2}{\sqrt{\pi}} \int_0^\xi \exp(-\xi^2) d\xi \quad (22b)$$

and the first derivative of equation (22b) is

$$\operatorname{erf}(\xi) d\xi = \frac{2}{\sqrt{\pi}} \exp(-\xi^2) d\xi \quad (22c)$$

Differentiation of equation (22a) with respect to ξ and the substitution of equation (22c) in the resulting expression yields

$$\frac{dc}{d\xi} = - \frac{c''_0 - c''_1}{2} \left[- \frac{2}{\sqrt{\pi}} \exp(-\xi^2) \right] \quad (22d)$$

Substitution of the original variable, x, in equation (22d) yields

$$\frac{dc}{dx} = \frac{c''_0 - c''_1}{2 \sqrt{\pi Dt}} \exp \left(- \frac{x^2}{4Dt} \right) \quad (23)$$

since, $d\xi = dx/2\sqrt{Dt}$.

APPENDIX IV

The Leeds & Northrup automatic recording microphotometer is shown in Plate III. This equipment consists of the plate stage, associated driving mechanism, the optical system, the amplifier, and the Speedomax recording unit.

The plate stage is designed to accommodate plates or films as large as 4" x 10", although films such as G.E. 1-7/8" x 16" may be used by scanning 24 cm and then moving the film to scan the remainder. Provision is also made for using the films or plates shorter than 10".

The stage is mounted on a compound plate carriage with provision for manual or synchronous movement in the horizontal direction, and manual movement in the vertical direction. The synchronous horizontal drive provides nine speeds: 0.1, 0.2, 0.5, 1., 2., 5., 10., 20., and 50. mm/minute.

The optical system used is of the highest quality available. On the photocell side of the plate, the lens system and the slit are rigidly coupled together, the whole being adjustable for focusing on the emulsion which is on the light source side of the plate. The light source is a straight filament lamp operated from storage batteries to insure the constancy of light output. The light together with its optical system is provided with suitable focusing adjustments for

focusing the filament image on the emulsion. The length of scanning light beam is adjustable, the range being approximately 1 to 2.5 millimeters.

The output of the photocell is applied to the Speedomax recorder by means of a conventional balanced tube amplifier.

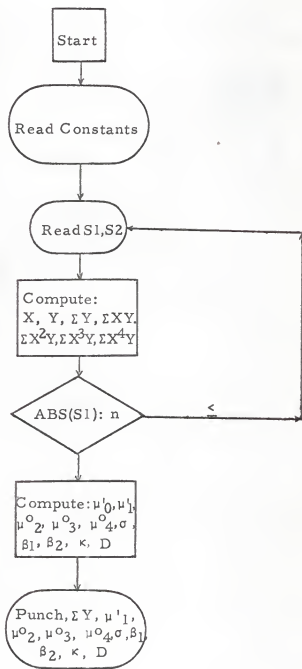
The record of the relative plate densities is drawn with ink on a chart paper. The chart is driven by a synchronous motor connected to the same supply as the synchronous motor driving the stage carriage, thus insuring a definite relation between the chart travel and plate travel. A special scale is furnished for reading plate motion in terms of millimeters of chart motion.

The Speedomax recorder carries an arbitrary uniform scale, 0 to 100 divisions. With the light shut off from the photocell the recorder is adjusted so that it reads at some major division near the low end of the scale. A spectrograph plate is put in the holder, and with an unexposed area set on the optical axis the lamp voltage is adjusted until the recorder reads a major division at or near the top of the scale. Deflections between the dark zero and the maximum light through the unexposed section of the plate are linear with transmitted light.

In this study the transparency was sandwiched between two glass plates and then mounted on the plate stage. After adjusting the dark zero and the maximum light through the unexposed section

of transparency on the Speedomax recorder, the transparency was scanned along the reference line A-A', at the plate speed of 10 millimeters/minute. The chart speed was preset at 6"/minute. Along the reference line A-A', when a fringe crossed the reference line, a peak in the dark side of the scale was recorded. The distances between the successive dark peaks were then, the distances between the successive fringes.

APPENDIX V

Flow Sheet and Computer Program for Statistical Treatment of Data

COMPUTER PROGRAM

C C TO EVALUATE STD. DEV., ROMESH AMIN, RUN ,

SUMY = 0.0

SUMXY = 0.0

SUMX2 = 0.0

SUMX3 = 0.0

SUMX4 = 0.0

A1 = 4.0

A2 = 3.0

A3 = 2.0

A5 = 1.0

A6 = 6.0

A7 = 16.0

A8 = 12.0

A9 = 9.0

T = 200.

TNI = 1.0

DEL = 0.0286

GAM = 33.55

7 READ, S1, S2

X = S1/GAM

Y = S2*GAM*DEL

$$\text{SUMY} = \text{SUMY} + \text{Y}$$

$$\text{SUMXY} = \text{SUMXY} + \text{Y} * \text{X}$$

$$\text{SUMX2} = \text{SUMX2} + \text{Y} * \text{X} * \text{X}$$

$$\text{SUMX3} = \text{SUMX3} + \text{Y} * \text{X} * \text{X} * \text{X}$$

$$\text{SUMX4} = \text{SUMX4} + \text{Y} * \text{X} * \text{X} * \text{X} * \text{X}$$

IF (ABS(S1) - 30.) 9, 9, 11

9 GO TO 7

$$11 \text{UM11} = \text{SUMXY} / \text{SUMY}$$

$$\text{UM12} = \text{SUMX2} / \text{SUMY}$$

$$\text{UM13} = \text{SUMX3} / \text{SUMY}$$

$$\text{UM14} = \text{SUMX4} / \text{SUMY}$$

$$\text{UM2} = \text{UM12} - \text{UM11} ** 2.0$$

$$\text{UM3} = \text{UM13} - \text{A2} * \text{UM11} * \text{UM12} + \text{A3} * (\text{UM11} ** 3.0)$$

$$\text{UM4} = \text{UM14} - \text{A1} * \text{UM11} * \text{UM13} + \text{A6} * \text{UM12} * (\text{UM11} ** 2.0) - \text{UM12} * (\text{UM11} ** 4.)$$

$$\text{UM20} = \text{UM2} * (\text{TNI} ** 2.0)$$

$$\text{UM30} = \text{UM3} * (\text{TNI} ** 3.0)$$

$$\text{UM40} = \text{UM4} * (\text{TNI} ** 4.0)$$

$$\text{SIGMA} = \text{UM20} ** 0.50$$

$$\text{BETA1} = (\text{UM30} ** 2.) / (\text{UM20} ** 3.)$$

$$\text{BETA2} = (\text{UM40}) / (\text{UM20} ** 2.)$$

$$\text{C1} = \text{BETA1} * (\text{BETA2} ** 2.) + \text{A6} * \text{BETA1} * \text{BETA2} + \text{A9} * \text{BETA1}$$

$$\text{C2} = \text{A7} * \text{A3} * (\text{BETA2} ** 2.) - \text{A7} * \text{A2} * \text{BETA1} * \text{BETA2} - \text{A7} * \text{A6} * \text{BETA2}$$

$C3 = -A8 * A3 * BETA1 * BETA2 + A8 * A2 * BETA1 * BETA1 + A8 * A6 * BETA1$

$APPAK = (C1) / (C2 + C3)$

$DC = UM20 / T$

PUNCH, T, SUMY, UM20, UM30, UM40

PUNCH, SIGMA, BETA1, BETA 2, APPAK

PUNCH, DC

END

Nomenclature used in the computer program:

$$\text{SUMY} = \Sigma Y$$

$$\text{SUMXY} = \Sigma (Y \times X)$$

$$\text{SUMX2} = \Sigma (Y \times X \times X)$$

$$\text{SUMX3} = \Sigma (Y \times X \times X \times X)$$

$$\text{SUMX4} = \Sigma (Y \times X \times X \times X \times X)$$

$$T = 2t'$$

TNI = Width of the successive chords on abscissa

$$\text{DEL} = n_2 - n_1$$

GAM = Magnification power of the microscope

$$\text{UM11} = \mu'_1$$

$$\text{UM12} = \mu'_2$$

$$\text{UM13} = \mu'_3$$

$$\text{UM14} = \mu'_4$$

$$\text{UM2} = \mu_2$$

$$\text{UM3} = \mu_3$$

$$\text{UM4} = \mu_4$$

$$\text{UM20} = \mu^0_2$$

$$\text{UM30} = \mu^0_3$$

$$\text{UM40} = \mu^0_4$$

$$\text{SIGMA} = \sigma$$

$$\text{BETA1} = \beta_1$$

BETA2 = β_2

APPAK = K

DC = D'

APPENDIX VI

Sample Data Sheet and Sample Calculations

A sample data-sheet for the observation made at $t' = 60$ seconds in Run 1 is presented in Table 6. The distance x in this table is the actual distance on the optical wedge diffusion cell. This distance x was obtained by dividing the microphotometer reading by the magnification power of the microscope which was 33.55 in this case. The value of $\Delta n = n_2 - n_1$, the difference between the refractive indice of the two diffusing sucrose solutions was obtained from the Handbook of Physics and Chemistry (5). From these data, dn/dx , the refractive index gradient and x_{avg} , the arithmetic mean distance between two successive fringes were computed on a desk calculator.

The refractive index gradient thus obtained was plotted against x_{avg} , the arithmetic mean of the distance between two successive fringes. A smooth curve was drawn through these points, and an arbitrary origin (centroidal axis) was chosen. The base line was divided into chords of 0.0298 millimeter and numbered outward from the arbitrary axis. The various moments described previously were calculated with the help of the computer program presented in Appendix V and are presented in Table 7. The true centroidal axis was computed with the help of equation (29d).

The computed γ was obtained by the use of the Z-column of Sheppard table included in the Tables for Statisticians and Biometricians (12). The maximum ordinate of the computed curve was obtained from the relation

$$H_m = \frac{N}{\sigma \sqrt{2\pi}} = \frac{11.969}{\sqrt{2\pi} (0.45604)} = 0.3120 \quad (46)$$

where, H_m is the maximum ordinate at $x = 0$, and N is the cumulative frequency given by equation (29a). Various x 's, the distance from the centroidal axis were transferred into Z by the following relation

$$Z = \frac{x}{\sigma} = \frac{x}{0.45604} \quad (47)$$

For the obtained value of Z , the Z-column in Sheppard table gave the ordinate based on the unit value of the maximum ordinate H_m . The actual ordinate was computed from the following relation

$$H_i = \sqrt{2\pi} (H_m)(T_i) \quad (48)$$

where H_i is the ordinate corresponding to x_i , H_m is the maximum ordinate, and T_i is the value of ordinate obtained from the Sheppard Table based on the unit height of the maximum ordinate. H_i was plotted against x_i , and a smooth curve was drawn to obtain the computed distribution curve.

Table 6. Data-sheet for $t' = 60$ seconds in Run 1. x is the actual distance on the optical wedge diffusion cell. x_{avg} is the arithmetic mean of the distances between three successive fringes crossing the reference line.

x in mm	:	x in mm	:	dn/dx	:	x_{avg} in mm
0.0		0.2455		0.1158		0.1227
0.2455		0.1895		0.1503		0.3403
0.4350		0.1528		0.1861		0.5140
0.5878		0.1182		0.2403		0.6469
0.7060		0.1000		0.2842		0.7560
0.8060		0.0963		0.2953		0.8543
0.9023		0.0947		0.3023		0.9496
0.9970		0.0923		0.3081		1.0432
1.0893		0.0954		0.2981		1.1365
1.1847		0.1000		0.2843		1.2347
1.2847		0.1032		0.2749		1.3363
1.3879		0.1212		0.2339		1.4465
1.5051		0.1366		0.2078		1.5754
1.6457		0.2490		0.1143		1.7702
1.8943						

Table 7. Various moments and statistics computed with IBM 1620 computer for the observation at $t' = 60$ seconds in Run 1. The symbols and their meaning are the same as those used in the section "The calculation of diffusion coefficient".

$$\mu'_0 = 11.9690$$

$$\mu'_1 = -0.041002$$

$$\mu^0_2 = 0.19263$$

$$\mu^0_3 = 0.20798$$

$$\mu^0_4 = 0.012064$$

$$\sigma = 0.45604$$

$$\beta_1 = 0.020362$$

$$\beta_2 = 2.9180$$

$$K = -0.00780$$

MEASUREMENT OF DIFFUSION COEFFICIENT
USING LASER INTERFEROMETRIC TECHNIQUE

by

ROMESHBHAI V. AMIN

B. Sc., Maharaja Sayajirao University, 1959

B. S., University of Missouri School of
Mines and Metallurgy, 1962

AN ABSTRACT OF THE MASTER'S THESIS

submitted in partial fulfillment of the
requirements of the degree

MASTER OF SCIENCE

Department of Chemical Engineering

KANSAS STATE UNIVERSITY

Manhattan, Kansas

1966

ABSTRACT

The purpose of this work was to set up the photomicrographic equipment necessary for the determination of the binary liquid diffusion coefficient and the measurement of these coefficient for an aqueous sucrose solution. These coefficients were measured by the determination of the refractive index gradient using an interferometric optical wedge diffusion cell.

A parallel monochromatic light source from a laser was used to obtain the interference fringe pattern between the two diffusing liquids contained in the diffusion cell. This interference fringe pattern was magnified with a microscope and then photographed at increasing time intervals. The refractive index gradient curve was obtained from the measurements of distances between successive fringes crossing the reference line.

The diffusion coefficient was computed from the refractive index gradient curve on the assumption that in the ideal case, the said curve has the properties of the Gaussian distribution curve. The coefficient thus obtained was corrected for the zero-time correction.

Experimental investigations were conducted to obtain the diffusion coefficient at one concentration of sucrose in aqueous solution. This coefficient was measured for an intermediate concentration of sucrose.

The experimental diffusion coefficient was compared with the values of the diffusion coefficient predicted from the previous studies in the extremely dilute and supersaturated sucrose concentration ranges. This comparison suggested that the concentration-dependence of the diffusion coefficient was curvilinear instead of linear in the intermediate sucrose concentration range.